Supplemental Materials

Molecular Biology of the Cell

Gnazzo et al.

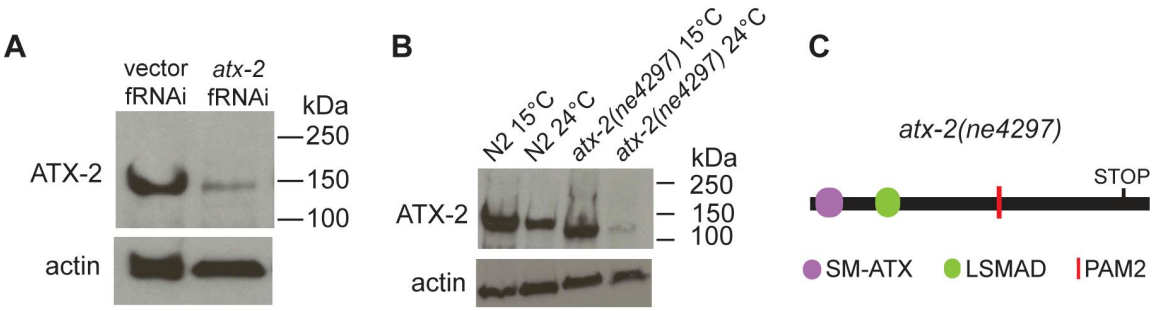

Figure S1: ATX-2 levels are decreased in *atx-2* fRNAi and *atx-2(ne4297)* embryos.

(A) Western blot analysis of ATX-2 expression levels in control (vector fRNAi) and *atx-2* fRNAi-treated embryos. Anti-actin (C4) was used as a loading control. (B) Western blot analysis of ATX-2 expression in the *atx-2(ne4297)* strain at the restrictive (24°C) temperature. ATX-2 expression levels in N2 and *atx-2(ne4297)* embryos grown at permissive (15°C) or restrictive (24°C) conditions. Anti-actin (C4) was used as a loading control. (C) The *atx-2(ne4297)* strain was sequenced and confirmed to contain a stop codon at Q919 of the *atx-2* gene.

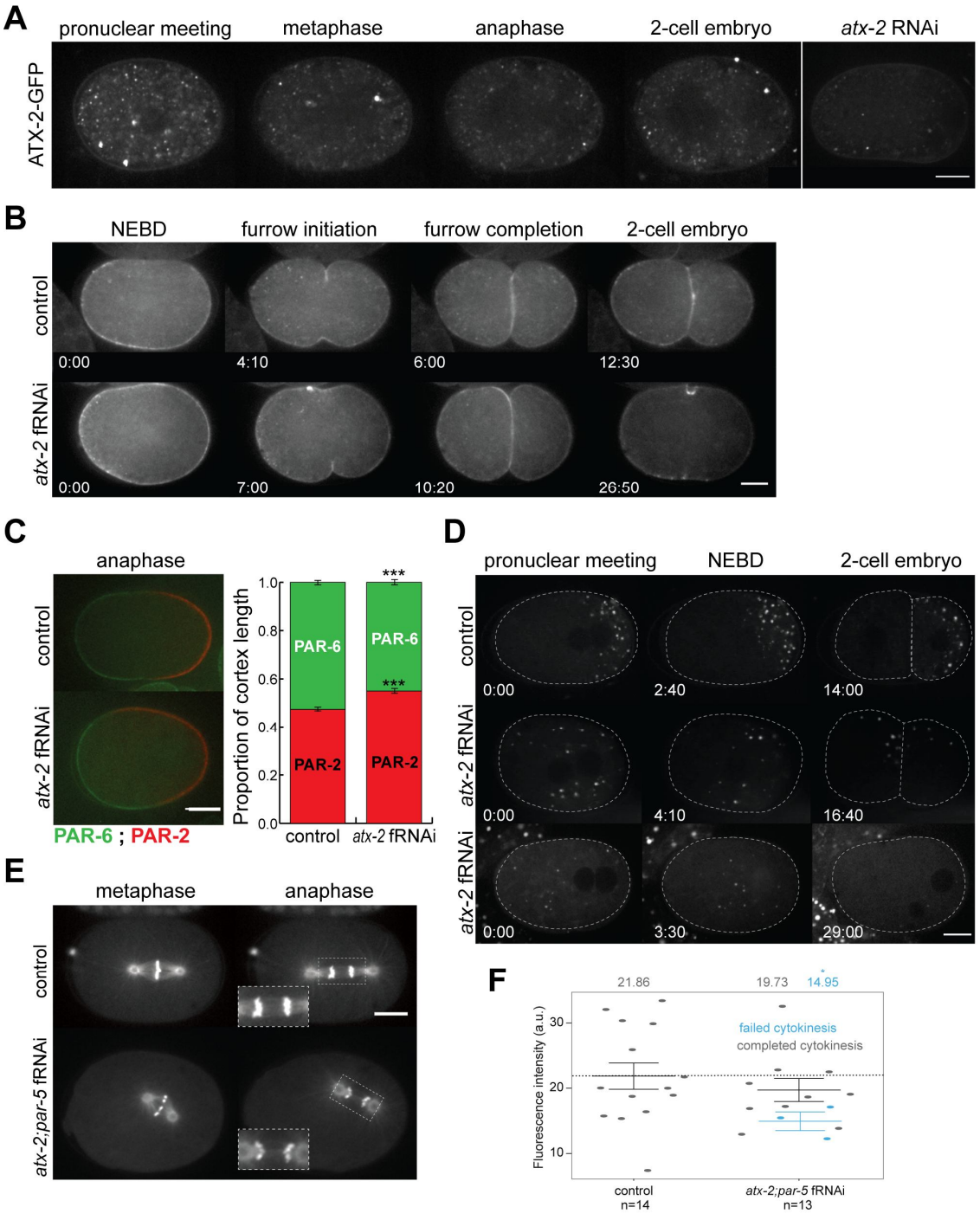
A
pronuclear meeting
metaphase
anaphase
2-cell embryo
atx-2 RNAi
ATX-2-GFP
B
NEBD
furrow initiation
furrow completion
2-cell embryo
control
atx-2 fRNAi
0:00
4:10
6:00
12:30
0:00
7:00
10:20
26:50
C
anaphase
control
atx-2 fRNAi
PAR-6 ; PAR-2
Proportion of cortex length
PAR-6
PAR-2
***
control
atx-2 fRNAi
D
pronuclear meeting
NEBD
2-cell embryo
control
atx-2 fRNAi
0:00
2:40
14:00
0:00
4:10
16:40
0:00
3:30
29:00
E
metaphase
anaphase
control
atx-2;par-5 fRNAi
F
21.86
19.73
14.95
failed cytokinesis
completed cytokinesis
Fluorescence intensity (a.u.)
control
n=14
atx-2;par-5 fRNAi
n=13

Figure S2: ATX-2 localization and depletion disrupts PAR proteins and P-granule segregation.

(A) Time-lapse confocal microscopy of an embryo expressing ATX-2-GFP from nuclear envelope breakdown (NEBD) to 2-cell. ATX-2 localizes to cytoplasmic puncta. Depletion of ATX-2 by fRNAi reduces the GFP signal observed. Scale bar, 10 μm. **(**B) Actin dynamics during the first cell division in control and *atx-2* fRNAi-treated embryos that express the actin marker MOE-1-GFP. In control embryos, the actin contractile ring assembles and contracts as the cell divides (6:00). The actin ring assembles in ATX-2 depleted embryos (10:20) and retracts as the cleavage furrow regresses (26:50). Accumulations of actin remain at the plasma membrane following cytokinesis failure (26:50). No further defects in actin ring assembly are observed. Times, in min:sec, are given relative to pronuclear meeting. (C) PAR-6 and PAR-2 domains are disrupted in *atx-2* fRNAi-treated embryos. Left: Control and *atx-2* fRNAi-treated embryos co-express GFP-PAR-2 and mCherry-PAR-6. Right: Quantification of the proportion of cortex length occupied by PAR-2 and PAR-6 in control (n=8) and *atx-2* fRNAi-treated (n=10) embryos at anaphase. Asterisks indicate statistical significance for compared data (p-value<0.001; Welch's *t*-test). Results are mean ± SEM. Times, in min:sec, are given relative to pronuclear meeting. (D) P-granule dynamics in control and in two *atx-2* fRNAi-treated embryos expressing GFP-PGL-1, one that completes cytokinesis and the other that fails. Images are maximum projections of 0.5 μm Z-stacks spanning 1.5 μm. In control embryos, the P-granules segregate to the posterior by pronuclear meeting (0:00) and maintain a posterior localization into the 2-cell stage (14:00). In *atx-2* fRNAi embryos, the P-granules do not completely segregate to the posterior at pronuclear meeting (0:00) and these puncta persist in the AB cell at the 2-cell stage (16:40). Scale bar, 10 μm. (E) Microtubule dynamics in control and *atx-2;par-5* fRNAi-treated embryos co-expressing TBB-2-GFP and GFP-HIS-11 in metaphase and anaphase. Insets show 1.5X-magnified view of spindle midzone microtubules in dashed boxes. Control embryos contain midzone microtubules and *atx-2;par-5* fRNAi-treated embryos show faint midzone microtubules. Scale bar, 10 μm. (F) Quantification of TBB-2-GFP fluorescence intensity in control and *atx-2;par-5* fRNAi-treated embryos. Fluorescence intensity was measured by drawing a region of interest between the dividing chromosomes in anaphase. Each point represents a fluorescence intensity measurement from a single embryo. Grey points represent embryos in which cytokinesis successfully completed; blue points represent embryos in which cytokinesis failed to complete. Reduced TBB-2-GFP fluorescence intensity at the spindle midzone was observed in ATX-2; PAR-5 depleted embryos. Solid lines denote the mean. Results are the mean ± SEM. Asterisks represent level of significance for compared data. *p<0.05 (Welch's *t*-test).

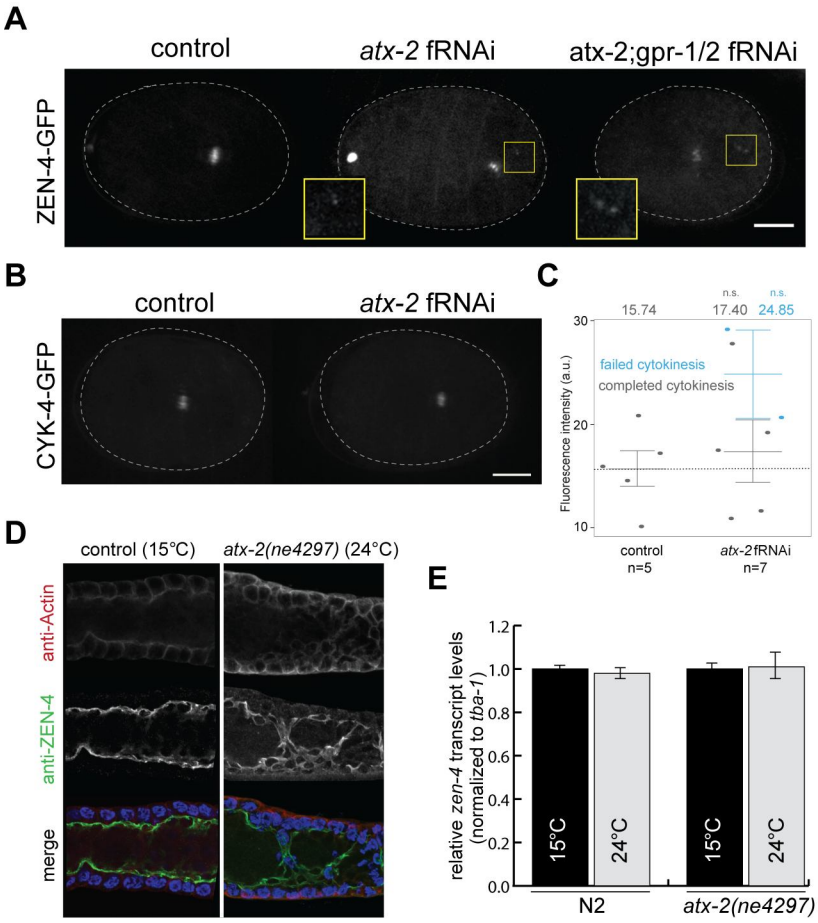

Figure S3: ATX-2 depletion disrupts ZEN-4 in germline but does not alter *zen-4* mRNA expression.

(A) ZEN-4-GFP localization in control, *atx-2* fRNAi-, and *atx-2; gpr-2* fRNAi-treated live anaphase staged embryos. In control embryos, ZEN-4 localizes to the spindle midzone. In *atx-2* fRNAi- and *atx-2; gpr-2* fRNAi-treated embryos ZEN-4 expression at the midzone is reduced and ectopic expression of ZEN-4 is observed in the embryo posterior within proximity to the posterior centrosome. Images are maximum projections of 0.5 µm Z-stacks spanning 1.5 µm. Scale bars, 10 µm. (B) CYK-4-GFP localization in control and *atx*-2 fRNAi-treated live anaphase stages embryos. In both control and *atx-2* fRNAi-treated embryos CYK-4-GFP localizes to the spindle midzone. Images are maximum projections of 0.5 µm Z-stacks spanning 1.5 µm. Scale bars, 10 µm. (C) Quantification of CYK-4-GFP fluorescence intensity in control and *atx-2; par*-5 fRNAi-treated embryos. Each point represents a fluorescence intensity measurement from a single embryo. Grey points represent embryos in which cytokinesis successfully completed; blue points represent embryos in which cytokinesis failed to complete. Co-depletion of ATX-2 and PAR-5 does not rescue the ATX-2 single depletion phenotype. Solid lines denote the mean. Results are the mean ± SEM. (D) ZEN-4 localization in *atx-2(ne4297)* germlines at a permissive (15°C) or restrictive (24°C) temperature. Dissected germlines are fixed and stained with

anti-Actin (red), anti-ZEN-4 serum (green), and DAPI (blue). In control germlines, ZEN-4 localizes along with actin at the rachis periphery. In ATX-2 depleted germlines, ZEN-4 localization moves away from the cellular junction and distributes throughout the rachis. This mislocalization appears to correlate with failures in germline cytokinesis, as observed by the absence of T-shaped cellular junctions with the actin staining. Images are projections of 0.2 µm Z-stacks spanning 6.2 µm. Scale bar, 10 µm. (E) qPCR analysis of the relative transcript expression levels of *zen*-4 in control and *atx-2(ne4297)* worms grown either at 15°C or 24°C. mRNA levels were normalized to *tba-1* (α-tubulin) and 24°C samples were compared to their respective 15°C control sample. *zen*-4 mRNA expression is unchanged when ATX-2 is depleted. Results are mean ± SEM.